ACS SENSORS

Article

Cite This: ACS Sens. 2019, 4, 1306−1312

pubs.acs.org/acssensors

Development of Label-Free Colorimetric Assay for MERS-CoV Using Gold Nanoparticles

Hanbi Kim,[†,¶] Minseon Park,[†,‡,¶] Joonki Hwang,[†,●] Jin Hwa Kim,[†] Doo-Ryeon Chung,[§,∥,⊥] Kyu-sung Lee,[*,†,‡,#] and Minhee Kang[*,†,‡]

[†]Smart Healthcare & Device Research Center and [§]Center for Infection Prevention and Control, Samsung Medical Center, Seoul, Korea

[‡]Department of Medical Device Management and Research, SAIHST (Samsung Advanced Institute for Health Sciences & Technology), Sungkyunkwan University, Seoul, Korea

[∥]Asia Pacific Foundation for Infectious Diseases (APFID), Seoul, Korea

[⊥]Division of Infectious Diseases, Department of Internal Medicine and [#]Department of Urology, Samsung Medical Center, Sungkyunkwan University School of Medicine, Seoul, Korea

Supporting Information

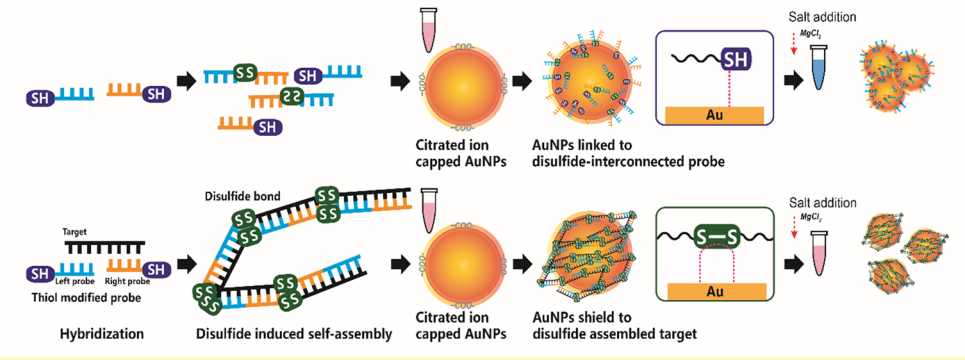

ABSTRACT: Worldwide outbreaks of infectious diseases necessitate the development of rapid and accurate diagnostic methods. Colorimetric assays are a representative tool to simply identify the target molecules in specimens through color changes of an indicator (e.g., nanosized metallic particle, and dye molecules). The detection method is used to confirm the presence of biomarkers visually and measure absorbance of the colored compounds at a specific wavelength. In this study, we propose a colorimetric assay based on an extended form of double-stranded DNA (dsDNA) self-assembly shielded gold nanoparticles (AuNPs) under positive electrolyte (e.g., 0.1 M $MgCl_2$) for detection of Middle East respiratory syndrome coronavirus (MERS-CoV). This platform is able to verify the existence of viral molecules through a localized surface plasmon resonance (LSPR) shift and color changes of AuNPs in the UV−vis wavelength range. We designed a pair of thiol-modified probes at either the 5′ end or 3′ end to organize complementary base pairs with upstream of the E protein gene (upE) and open reading frames (ORF) 1a on MERS-CoV. The dsDNA of the target and probes forms a disulfide-induced long self-assembled complex, which protects AuNPs from salt-induced aggregation and transition of optical properties. This colorimetric assay could discriminate down to 1 pmol/μL of 30 bp MERS-CoV and further be adapted for convenient on-site detection of other infectious diseases, especially in resource-limited settings.

KEYWORDS: *colorimetric assay, Middle East respiratory syndrome coronavirus (MERS-CoV), molecular diagnosis, gold nanoparticle, label-free detection*

The point-of-care testing (POCT) market of infectious disease represents promising and significant growth in the global *in vitro* diagnostics (IVD) industry.[1] There are several factors that are stimulating the demand for infectious disease POCT, including the increasing spread of human immunodeficiency virus (HIV), tuberculosis (TB), and malaria in developing countries, and the threat of emerging and re-emerging infectious diseases such as the Middle East respiratory syndrome (MERS), severe acute respiratory syndrome (SARS), ZIKA, a variety of influenza strains, and the West Nile virus.[2] Infectious diseases pose a significant risk to human health and has led to more than half of the deaths worldwide.[3] Additionally, widespread infectious diseases have caused a continuous increase in fatality rates in developing

Received: January 23, 2019
Accepted: May 7, 2019
Published: May 7, 2019

DOI: 10.1021/acssensors.9b00175
ACS Sens. 2019, 4, 1306−1312

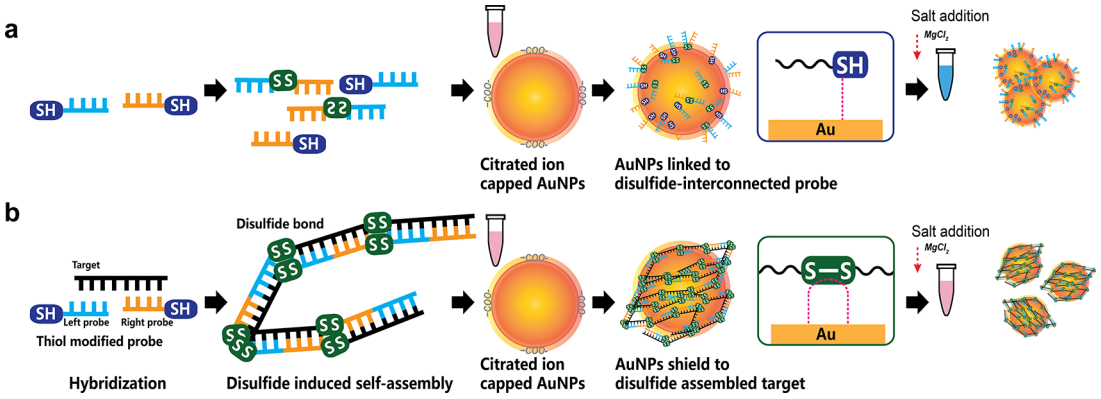

Figure 1. Colorimetric detection of DNA based on disulfide induced self-assembly. (a) Salt-induced aggregation of AuNPs in the absence of targets. (b) Procedures for preventing AuNPs from salt-induced aggregation by disulfide induced self-assembly in the presence of targets.

countries. The best way for containment of the epidemic is an early diagnosis, which is difficult using ordinary methods because of costly and large equipment, the necessity of experts, and slow data output.[4] Therefore, rapid POCT methods are crucial for overcoming these limitations by miniaturizing and reducing the device cost and providing simple, fast, easy-to-use diagnostic tests without specialized training.

Colorimetric detection originating from gold nanoparticles (AuNPs) have been intensively studied because of their particular optical properties, i.e., localized surface plasmon resonance (LSPR), which represent a color with maximal absorbance wavelength. AuNPs have been utilized in colorimetric assays for the detection of diverse biological molecules (e.g., proteins[5] and nucleic acids[6]) in that the change in particle color is generated by sensitive reactivity of nanosized particles to external condition. In addition, the disperse state is adjustably modified from artificial electrostatic force control by ion, pH, biomacromolecules, and so forth.[7,8] For example, a positive electrolyte (salt) causes metallic nanoparticle aggregation, causing a significant color change as a red-shift in the LSPR spectrum.[9,10] Based on that, a modified AuNP cross-linking method was demonstrated in Mirkin's group for DNA identification.[11] In the research, the surfaces of AuNPs were conjugated with two thiolated single-stranded DNA (ssDNA) via strong Au−S interactions. The hybridization of target DNAs with the ssDNAs on the surface of the AuNPs induces the formation of double-stranded DNA (dsDNA)-AuNP networks, resulting in AuNPs aggregation and dramatic color changes. The target DNA acts as a cross-linker between two ssDNA-functionalized AuNPs. On the other hand, colorimetric DNA sensing methods using functionalized AuNPs have been demonstrated using non-cross-linking DNA hybridization with the benefit of the powerful salting-out effect of dsDNA compared to ssDNA.[12] Since the ssDNA density on the surface of AuNPs and the ionic strength of the solution affect the stability of functionalized AuNPs, control of the aggregated state by modification is quite difficult in practical applications. Rothberg et al. suggested a label-free detection method based on the fact that ssDNA in the solution could bind to citrate-capped AuNPs and electrostatically stabilize them at high ionic strength. In such a system, AuNPs are stabilized in the presence of ssDNA, but aggregated with dsDNA in a highly concentrated electrolyte solution. This strategy does not need the direct binding of ssDNA on the surface of nanosized metallic particles, as the DNA amplification step prior to detection is inevitable due to the low sensitivity of this method.[13] Since both ssDNA and dsDNA allow AuNPs to stabilize at low salt concentration,[14−17] cationic agents are mainly used to identify the target with probes.[18,19] In this regard, Farhad Rezaee et al. demonstrated a modified non-cross-linking AuNP aggregation using disulfide self-assembly of terminal modified DNA. Long and flexible sulfur-rich, self-assembled products were well combined on the surface of AuNPs and effectively inhibit the particles from salt-induced aggregation.[15]

Inspired by this research, we developed a colorimetric assay that relies on bare AuNPs that employs a disulfide-induced self-assembly. The bare AuNP-based colorimetric method consists of two thiol modified probes at the 3′ or 5′ ends for targeting partial genomic regions (30 bp) of MERS-CoV along with upstream E protein gene (upE) and encoding open reading frames (ORF) 1a. This assay could be highly reliable for MERS-CoV diagnosis as we have followed WHO updated recommendations for infectious disease laboratory testing, which targets the two regions on MERS-CoV considered for potential preclinical screening and high sensitivity[20]

The developed assay platform was able to detect the target DNA through optical properties of the gold nanoparticles such as color changes with the naked eye and spectral shifts on UV−vis wavelength. The specific thiolated probes form the complementary dsDNA with the target and make a disulfide-induced long self-assembled complex due to continuous disulfide bond formation. The extended self-assembled complex can protect bare AuNPs for stability against salt-induced aggregation since sulfur-group at ends of dsDNA are mediated covalent bond with gold surface. The interaction is known to generate stable conjugation within disulfide-induced self-assembled complex and AuNPs and intermolecular force between Au−S attains about 40 to 50 kcal mol^{-1}.[21,22] Otherwise, probes build a disulfide induced interconnection with each other in the absence of targeting DNA. The probe DNA terminal coupling is unable to cover the surface of AuNPs exposed to aggregation, leading to significant color changes as well as a broader red-shift of the LSPR peak (Figure 1). With this method, we can visually observe the results with the naked eye, not using costly equipment. This colorimetric assay is an important step to use of infectious disease POCT across the developing world. Moreover, this concept of a disulfide bond based colorimetric assay could be applied for diagnosis of other infectious diseases.

DOI: 10.1021/acssensors.9b00175
ACS Sens. 2019, 4, 1306−1312

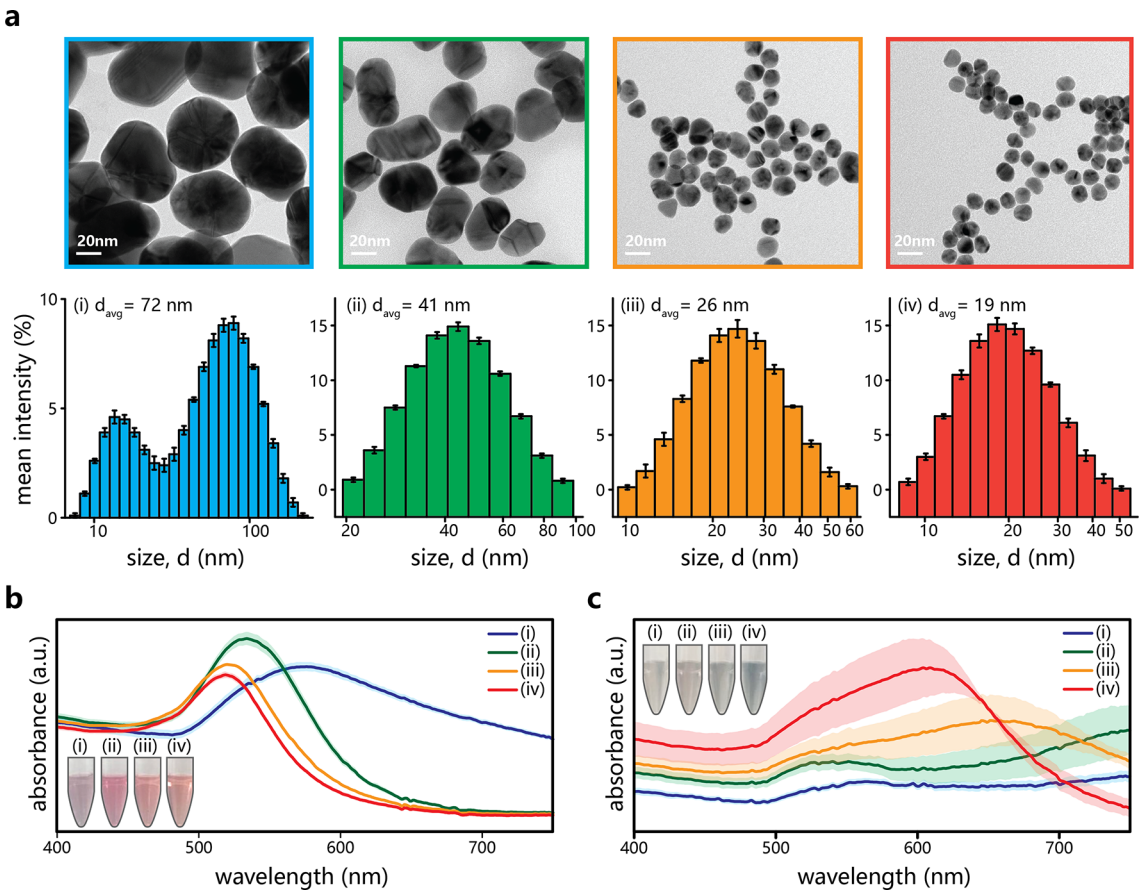

Figure 2. Morphological and optical properties of gold nanoparticles based on the synthesized conditions and electric charge in solution. (a) Size distribution of AuNPs measured from TEM images and DLS of gold nanoparticles (AuNPs). AuNPs, i.e., average size (iv) 19 nm, was used in this work. (b) UV−vis spectra of as-prepared AuNPs and (c) AuNPs after salt addition.

RESULTS AND DISCUSSION

Preparation of the Ideal Gold Nanoparticle upon a Spectral Centroid. We developed various sized gold nanoparticles for optimization as a colorimetric indicator. The citrate reduction method, i.e., Turkevich-Frens, is generally applied to synthesize stabilized gold nanoparticles under electrostatic repulsion.[23] Additionally, the ratio of the reducing agent and $HAuCl_4$ allow for the preparation of a diverse size of AuNPs. We changed the volume of trisodium citrate acid from 300 to 1600 μL to acquire different-sized AuNPs. The morphology of the prepared AuNPs and DLS records are reported in Figure 2a. According to the TEM images and DLS measurements, the average diameter of AuNPs decreased as the amount of trisodium citrate dehydrate increased. For instance, the addition of reducing agents (300, 500, 1200, 1600 μL) allow us to synthesize 72-, 41-, 26-, and 19-nm-sized gold nanospheres, respectively. This was the result of changed citrate and gold ratio to control the reduction and stabilization of the nanoparticle surface.[24,25] We optimized an average of 19 nm AuNP through reduction with 1600 μL of trisodium citrate and called that formed particle "bare gold", which means "unmodified and inartificial conjugation with any molecules after synthesized process" and "citrate ion capped gold nanoparticle derived from reduction and stabilization effects of sodium citrate" for this experiment. The structural and spectroscopic properties are presented as (iv) in Figure 2.

To evaluate the effects of salt on as-prepared AuNPs, the absorbance spectra of the bare AuNPs and those with $MgCl_2$ were measured using a conventional UV−visible spectrometer (Figure 2b,c). Since the LSPR spectral band of nanosized metallic particle is derived from dielectric factors, particle size and shape, the absorption peak shift indicated a changed environment surrounding AuNPs such as by conjugation of biomolecules. Thus, the addition of $MgCl_2$ induces a significant change in the absorption spectra. For example, the LSPR band has a decrease in intensity and increase in bandwidth, as well as new bands at longer wavelength. These LSPR band shifts represent the aggregation of AuNPs caused by the loss of interparticle repulsive force as salt disrupts the charge interaction surround AuNPs and promotes the interparticle van der Waals attractive forces.[26] As shown in the salt induced results, the solutions of gold nanoparticles, excluding 19 nm AuNPs, became gradually transparent due to severe aggregation of metal particles and also a broader, flattened spectra appeared in the UV−vis measurement as Figure 2c. Therefore, we selected the 19-nm-diameter AuNPs that detected the LSPR changes on the surface of the nanosized metallic particles in this experiment.

Furthermore, a spectral centroid was derived by calculating the centroid wavelength in each experiment spectrum to determine a credible and accurate point of the LSPR band. The spectral centroid represents several parameters of the LSPR band including the peak wavelength, bandwidth, and intensity that depend on the size, shape, concentration, and interparticle interactions of the AuNPs.[15,27] The shift of the centroid can be a comprehensive indicator for the overall transition of the

DOI: 10.1021/acssensors.9b00175
ACS Sens. 2019, 4, 1306−1312

spectral distribution toward shorter or longer wavelengths. For example, 19-nm-diameter AuNPs possess a spectral centroid at the orange-red wavelength 516 nm, whereas larger 72-nm-diameter AuNPs exhibit a purple color with a spectral centroid at 576 nm.

Optimization of Disulfide-Induced Long Self-Assembly and the Salting Agent. In this report, bare 19-nm-diameter AuNPs were used, and we selected a target and control upstream of the E protein gene (upE) and open reading frames (ORF) 1a on MERS-CoV, and the tobacco mosaic virus (TMV), respectively. Furthermore, we synthesized forward and reverse thiol modified probes specifically binding the target DNA and forming complementary base pairs. Each of the thiolated probes were modified at the 5′ site (Right: 5′R) and 3′ site (Left: 3′L). Once two probes simultaneously recognize a specific half of the target, the disulfide bonds at the 3′ and 5′ terminals readily form a sulfur-rich self-assembled complex. Specifically, target DNA samples were mixed with thiolated probes (5′ R, 3′ L) in distilled water (D.W.) and then incubated at 90 °C for a few minutes to establish disulfide-induced long self-assembled products. 90 μL of the AuNPs solution was then add to the above-mentioned mixture (60 μL). The solution was incubated at room temperature for 30 min and various amounts of $MgCl_2$ solutions were added. Each test was evaluated in at least triplicate.

We analyzed the color of the resulting solutions with the naked eye and UV−vis spectrometer. Disulfide self-assembled products were visualized along with the gel electrophoresis, where the presence of the target (positive reaction) displayed bands with a characteristic ladder due to the formation of long assemblies of dsDNA (Figure 3a). Polymorphous bands appeared with the formation of disulfide self-assembly between the target and probes on original full-length native polyacrylamide gel electrophoresis (PAGE) analysis image (Figure S1). Additionally, we confirm the sizes of DNA fragments with 4% agarose gel which is commonly used to separate and visualize the amplified DNA outcomes depended on number of base pairs (Figure S2).

Furthermore, we confirmed the adsorbed components on the surface of gold nanoparticle via X-ray photoelectron spectroscopy (XPS) (Figure 3b). In the case where thiolated probe met the incompatible DNA, the S_{2p} signals mainly indicated the absorbed thiol component at $S_{2p3/2}$ photoelectron binding energy (BE) of 162.2 eV since a sulfur monolayer was formed on the surface of AuNPs from the probe solution ($\overline{S}$, $S\overline{H}$, or SH_2 species) (Figure 3b(i)).[28,29] Meanwhile, XPS spectrum can be fitted at 163.37 and 164.55 eV of $S_{2p3/2}$ binding energy when target DNA and probes compose the disulfide-induced self-assembled multilayers on AuNPs (Figure 3b(ii)). The observed components at 163−164 eV of BE are assigned to some S in multilayer which highly defect to the gold surface or domain boundaries.[29,30] Although BE of 163.7 appeared in Figure 3b(i), the area in the XPS spectrum was lower than thiol species (1:0.64), and in PAGE, the size of DNA fragments only appeared close to 20 bp ladder that indicates thiol containing short layers formed, not the disulfide based multilayer, and unbound thiol assigned that BE of $S_{2p\ 3/2}$ when target DNA is absent.[31] Also, the increased area at higher binding energy indicates higher coverage with absorbed polysulfides.[22] Based on results mentioned earlier from PAGE and XPS analyses, disulfide-induced self-assembled complex composed the multilayers on AuNPs, but thiolated

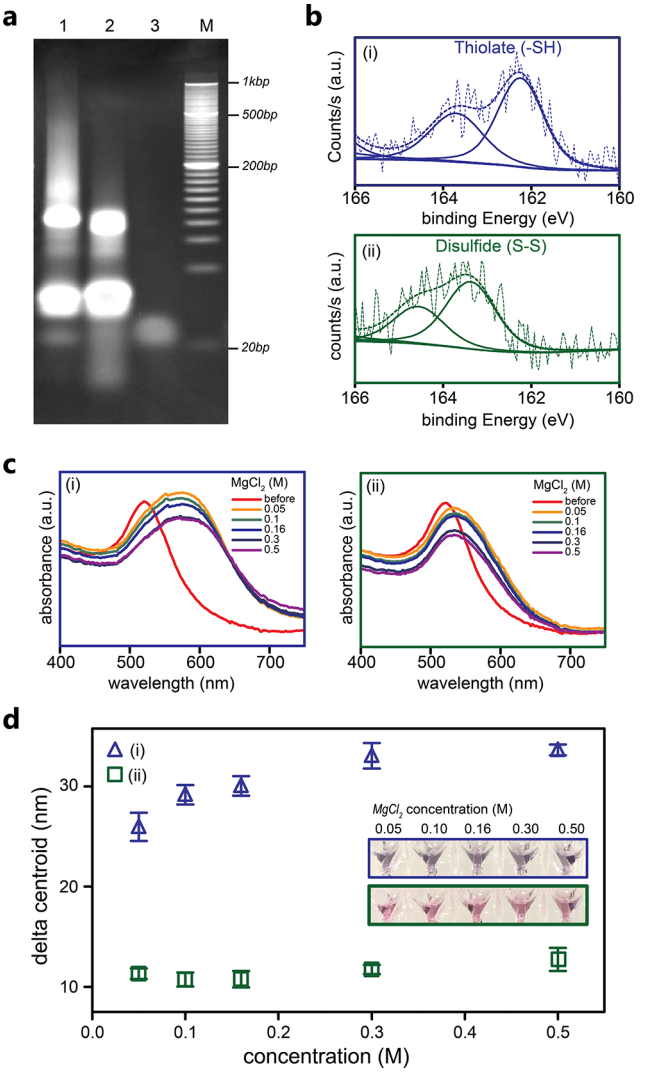

Figure 3. Visible results analysis depending on (i) negative (TMV) and (ii) positive control (ORF1a). (a) Native polyacrylamide gel electrophoresis (PAGE) analysis for confirmation of disulfide-induced self-assembly with target DNA and probes (lane 1: ORF1a, lane 2: upE), and nonextended result of negative control and equal probes with positive control (lane 3: TMV). (Figure S1 shows the original full-length native polyacrylamide gel electrophoresis (PAGE) analysis image.) (b) X-ray photoelectron spectroscopy (XPS) analysis depends on $S_{2p\ 3/2}$ binding energy for confirming the presence of sulfur group based layers on gold surface (162.2 eV: $\overline{S}$, $S\overline{H}$, or SH_2 species, 163.7 eV: thiol containing short layers, 163.37 and 164.55 eV: S multilayer). (c) Absorption spectra of AuNPs exposed to various concentrations of salt (0.05, 0.1, 0.16, 0.3, and 0.5 M of $MgCl_2$). (d) Spectral centroid shifts depending on the salt concentration.

ssDNA probes form monolayer which is hard to cover the surface of gold nanoparticle from salt-induced aggregation. DLS measurements also supported the size increasing of DNA covered AuNPs which depended on extended layers (Figure S3). Dynamic light scattering (DLS) was used to monitor the distribution of the hydrodynamic size of the gold nanoparticles after immobilized ssDNA or dsDNA complex layer on the gold surface, respectively. As shown in Figure S3, the average hydrodynamic size of the gold nanoparticle protected by disulfide-induced self-assembly from the positive reaction was increased by approximately 8.11 nm compared to immobilized ssDNA on gold nanoparticle from the negative reaction.

DOI: 10.1021/acssensors.9b00175
ACS Sens. 2019, 4, 1306−1312

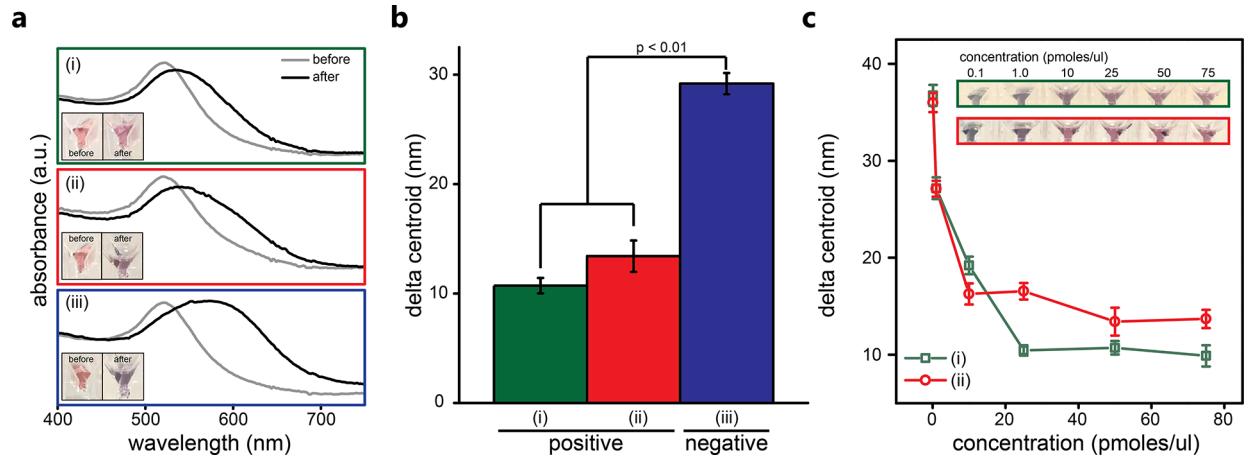

Figure 4. Spectral analysis of the colorimetric assay for detection of partial MERS-CoV including (i) ORF1a and (ii) upE and negative control of (iii) TMV. (a) UV−vis spectra of the AuNPs solution before and after adding salt in the presence or absence of disulfide-induced self-assembled targets. (b) Average delta centroid of positive controls and a negative control at 0.1 M MgCl2 ((i) avg. 10.7 nm, (ii) avg. 13.4 nm, (iii) avg. 29.1 nm)). (c) LOD graph of the positive control according to target concentration.

The stability of the assay was investigated through the addition of various concentrations of $MgCl_2$ into the bare AuNPs solution in the (i) absence or (ii) existence of the target (Figure 3c). Mixed products with target DNA and probe solutions shielded the particles, which tolerated the salting more than gold nanoparticles conjugated with thiol from disulfide-interconnected probes, since the disulfide-induced self-assembled complex was used to protect bare AuNPs against salt addition. The spectral peak of the AuNPs colloid was not quite different with bare AuNPs when the target DNA is in the solution with 0.05 to 0.5 M $MgCl_2$, while AuNPs linked to disulfide-interconnected probes aggregated with any concentration of salt. However, the absorbance declined slightly, corresponding to an increased salt concentration whether extended disulfide assemblies were formed or not. Therefore, the spectral centroid shifts depending on salt concentration were plotted and are shown in Figure 3d. At all concentrations (0.05 to 0.5 M), the delta centroid of the negative control showed more shift than positive controls due to intergold nanoparticle aggregation, while the centroid shift of the positive control was the smallest at 0.1 M of $MgCl_2$. As previously mentioned, the absorbance declined conversely according to the increase in salt concentration. Hence, 0.1 M of $MgCl_2$ was chosen as the optimized concentration.

Verification of the Colorimetric Assay. To consider the disulfide self-assembled reaction dependence on target DNAs and their concentrations, we measured the absorption change of the AuNP solution before and after adding 0.1 M $MgCl_2$ in the presence or absence of each target using a UV−vis spectrometer. When the target was absent, the wavelength was shifted more toward the red side of the spectrum compared to when the target was present. The wavelength peak shifts were 11, 19, and 51 nm after complementary binding reactions between probes and (i) ORF1a, (ii) upE, and (iii) TMV, respectively ((i) 522 to 533 nm, (ii) 520 to 541 nm, and (iii) 521 to 572 nm) (Figure 4a,b). Due to the broad spectrum of the negative control, delta centroid was estimated as 2.5 times greater than a positive reaction (avg. 29 nm vs avg 12 nm). These changes indicate that positive samples (ORF1a and upE) that are a mixture of thiol-modified probes and their target DNA that hindered the aggregation of AuNPs through composition of the long self-assembled structures. Negative samples (TMV) were unable to form long self-assembled structures due to mismatched targets. Furthermore, we calculated a *p*-value to prove the reproducibility of this colorimetric platform (Figure 4b). The *p*-value is the probability that might yield the same results observed in the biological study, if the null hypothesis is true. All data groups were found to pass the null-hypothesis assuming a normal distribution was followed.[32] Therefore, the *p*-value of the delta centroid implies that this assay is considered statistically significant (*p*-value <0.01).

The limit-of-detection (LOD) was determined in order to apply to the medical laboratory field. The LOD of this colorimetric platform was 1 pmol/μL, which was calculated by the equation $Mean_{blank} + 3\sigma_{blank}$ defined from the IUPAC standard (Figure 4c).[33] 1 pmol/μL is about 6×10^{11} copies/μL, which requires only 26 PCR cycles to diagnose MERS patients who release 1.5×10^3 to 6.7×10^3 copies/μL in the sputum for 10 days and have recovered without specific treatment for MERS-CoV. This assay can reduce the number of PCR cycles for diagnosis of MERS even with a small amount of viral molecules, compared to conventional PCR reactions that require more than about 34 cycles to detect MERS-CoV.[34−37]

CONCLUSIONS

A simple and fast colorimetric assay for detecting infectious disease that can be seen by the naked eye without costly equipment was developed. We proposed a colorimetric assay using disulfide bonds formed by hybridizing with thiolated probes and a target; this method inhibited the aggregation of AuNPs by salt and limits the color change for diagnosis of MERS. This assay can confirm the presence of MERS-CoV within 10 min without electrophoresis or other procedures. The assay could discriminate MERS-CoV with a potential detection limit of 1 pmol/μL, which means it could distinguish a lower amount of target with a lower level of amplification, or even without amplification. A follow-up study will be conducted to apply this method to clinical samples with longer targeting regions. We anticipate that this method will provide rapid and accurate diagnostic results in epidemic areas, especially in resource-limited settings and will evolve by

DOI: 10.1021/acssensors.9b00175
ACS Sens. 2019, 4, 1306−1312

combining with a mobile platform and artificial intelligence in the near future.

■ ASSOCIATED CONTENT

Supporting Information

The Supporting Information is available free of charge on the ACS Publications website at DOI: 10.1021/acssensors.9b00175.

PAGE analysis; Agarose gel electrophoresis analysis; Hydrodynamic size distribution measured by DLS; Experimental methods (PDF)

■ AUTHOR INFORMATION

Corresponding Authors

*E-mail: minikang@skku.edu.

*E-mail: minhee.kang@samsung.com.

ORCID

Minhee Kang: 0000-0003-0330-7828

Present Address

●J. Hwang: Life Science Laboratory, SG Medical, Seoul, Korea

Author Contributions

¶H. Kim and M. Park contributed equally to this work. The manuscript was written by contributions from all authors who have given approval to this final version of the manuscript.

Notes

The authors declare no competing financial interest.

■ ACKNOWLEDGMENTS

This research was supported by a grant of the Korea Health Technology R&D Project through the Korea Health Industry Development Institute (KHIDI), funded by the Ministry of Health & Welfare, Republic of Korea (HG18C0062, HI14C3229) and the Bio & Medical Technology Development Program of the National Research Foundation (NRF) funded by the Ministry of Science (2016M3A9B6919189).

■ REFERENCES

(1) Who Mers-Cov Research, G.. State of Knowledge and Data Gaps of Middle East Respiratory Syndrome Coronavirus (MERS-CoV) in Humans. *PLoS Curr.* **2013**, 1.

(2) *MediPoint: Point of Care Diagnostics - Global Analysis and Market Forecasts* 2016; pp 1−187.

(3) Morens, D. M.; Fauci, A. S. Emerging infectious diseases: threats to human health and global stability. *PLoS Pathog.* **2013**, *9* (7), e1003467.

(4) Tallury, P.; Malhotra, A.; Byrne, L. M.; Santra, S. Nanobioimaging and sensing of infectious diseases. *Adv. Drug Delivery Rev.* **2010**, *62* (4−5), 424−437.

(5) Kim, J. W.; Kim, J. H.; Chung, S. J.; Chung, B. H. An operationally simple colorimetric assay of hyaluronidase activity using cationic gold nanoparticles. *Analyst* **2009**, *134* (7), 1291−1293.

(6) Huang, P.; Wang, H. L.; Cao, Z. G.; Jin, H. L.; Chi, H.; Zhao, J. C.; Yu, B. B.; Yan, F. H.; Hu, X. X.; Wu, F. F.; Jiao, C. C.; Hou, P. F.; Xu, S. N.; Zhao, Y. K.; Feng, N.; Wang, J. Z.; Sun, W. Y.; Wang, T. C.; Gao, Y. W.; Yang, S. T.; Xia, X. Z. A Rapid and Specific Assay for the Detection of MERS-CoV. *Front. Microbiol.* **2018**, 1 DOI: 10.3389/fmicb.2018.01101.

(7) Sastry, M.; Rao, M.; Ganesh, K. N. Electrostatic assembly of nanoparticles and biomacromolecules. *Acc. Chem. Res.* **2002**, *35* (10), 847−855.

(8) Verveniotis, E.; Kromka, A.; Ledinsky, M.; Cermak, J.; Rezek, B., Guided assembly of nanoparticles on electrostatically charged nanocrystalline diamond thin films. *Nanoscale Res. Lett.* **2011**, DOI: 10.1186/1556-276X-6-144.

(9) Willets, K. A.; Van Duyne, R. P. Localized surface plasmon resonance spectroscopy and sensing. *Annu. Rev. Phys. Chem.* **2007**, *58*, 267−97.

(10) Abbas, A.; Kattumenu, R.; Tian, L.; Singamaneni, S. Molecular linker-mediated self-assembly of gold nanoparticles: understanding and controlling the dynamics. *Langmuir* **2013**, *29* (1), 56−64.

(11) Elghanian, R.; Storhoff, J. J.; Mucic, R. C.; Letsinger, R. L.; Mirkin, C. A. Selective colorimetric detection of polynucleotides based on the distance-dependent optical properties of gold nanoparticles. *Science* **1997**, *277* (5329), 1078−1081.

(12) Fennell Evans, H. W. *The colloidal domain: Where physics, chemistry, biology, and technology meet*, 2nd ed.; Wiley-VCH: 1999.

(13) Valentini, P.; Pompa, P. P. Gold nanoparticles for naked-eye DNA detection: smart designs for sensitive assays. *RSC Adv.* **2013**, *3* (42), 19181−19190.

(14) Li, H.; Rothberg, L. J. Label-free colorimetric detection of specific sequences in genomic DNA amplified by the polymerase chain reaction. *J. Am. Chem. Soc.* **2004**, *126* (35), 10958−61.

(15) Shokri, E.; Hosseini, M.; Davari, M. D.; Ganjali, M. R.; Peppelenbosch, M. P.; Rezaee, F. Disulfide-induced self-assembled targets: A novel strategy for the label free colorimetric detection of DNAs/RNAs via unmodified gold nanoparticles. *Sci. Rep.* **2017**, *7*, 1 DOI: 10.1038/srep45837.

(16) Li, H.; Rothberg, L. Colorimetric detection of DNA sequences based on electrostatic interactions with unmodified gold nanoparticles. *Proc. Natl. Acad. Sci. U. S. A.* **2004**, *101* (39), 14036−14039.

(17) Wang, L.; Liu, X.; Hu, X.; Song, S.; Fan, C. Unmodified gold nanoparticles as a colorimetric probe for potassium DNA aptamers. *Chem. Commun.* **2006**, No. 36, 3780−3782.

(18) Polavarapu, L.; Xu, Q.-H. J. L. *Langmuir* **2008**, *24* (19), 10608−10611.

(19) Xia, F.; Zuo, X.; Yang, R.; Xiao, Y.; Kang, D.; Vallée-Bélisle, A.; Gong, X.; Yuen, J. D.; Hsu, B. B.; Heeger, A. J. *Proc. Natl. Acad. Sci. U. S. A.* **2010**, *107* (24), 10837−10841.

(20) W. W. H. Organization, Laboratory testing for Middle East Respiratory Syndrome Coronavirus Interim guidance; https://www.who.int/csr/disease/coronavirus_infections/mers-laboratory-testing/en/.

(21) Li, F.; Zhang, H.; Dever, B.; Li, X. F.; Le, X. C. Thermal stability of DNA functionalized gold nanoparticles. *Bioconjugate Chem.* **2013**, *24* (11), 1790−1797.

(22) Pensa, E.; Cortes, E.; Corthey, G.; Carro, P.; Vericat, C.; Fonticelli, M. H.; Benitez, G.; Rubert, A. A.; Salvarezza, R. C. The chemistry of the sulfur-gold interface: in search of a unified model. *Acc. Chem. Res.* **2012**, *45* (8), 1183−1192.

(23) Frens, G. Controlled Nucleation for the Regulation of the Particle Size in Monodisperse Gold Suspensions. *Nature, Phys. Sci.* **1973**, *241*, 20−22.

(24) Sau, T. K.; Pal, A.; Jana, N. R.; Wang, Z. L.; Pal, T. Size controlled synthesis of gold nanoparticles using photochemically prepared seed particles. *J. Nanopart. Res.* **2001**, *3* (4), 257−261.

(25) Kimling, J.; Maier, M.; Okenve, B.; Kotaidis, V.; Ballot, H.; Plech, A. Turkevich method for gold nanoparticle synthesis revisited. *J. Phys. Chem. B* **2006**, *110* (32), 15700−15707.

(26) Zhao, W.; Brook, M. A.; Li, Y. F. Design of Gold Nanoparticle-Based Colorimetric Biosensing Assays. *ChemBioChem* **2008**, *9* (15), 2363−2371.

(27) Dahlin, A. B.; Chen, S.; Jonsson, M. P.; Gunnarsson, L.; Kall, M.; Höök, F. J. A. c. *Anal. Chem.* **2009**, *81* (16), 6572−6580.

(28) Lustemberg, P. G.; Vericat, C.; Benitez, G. A.; Vela, M. E.; Tognalli, N.; Fainstein, A.; Martiarena, M. L.; Salvarezza, R. C. Spontaneously formed sulfur adlayers on gold in electrolyte solutions: Adsorbed sulfur or gold sulfide? *J. Phys. Chem. C* **2008**, *112* (30), 11394−11402.

(29) Vericat, C.; Vela, M. E.; Andreasen, G.; Salvarezza, R. C.; Vazquez, L.; Martin-Gago, J. A. Sulfur-substrate interactions in

spontaneously formed sulfur adlayers on Au(111). *Langmuir* **2001**, *17* (16), 4919−4924.
(30) Koczkur, K. M.; Hamed, E. M.; Houmam, A. Sulfur multilayer formation on Au(111): new insights from the study of hexamethyldisilathiane. *Langmuir* **2011**, *27* (20), 12270−4.
(31) Castner, D. G.; Hinds, K.; Grainger, D. W. X-ray photoelectron spectroscopy sulfur 2p study of organic thiol and disulfide binding interactions with gold surfaces. *Langmuir* **1996**, *12* (21), 5083−5086.
(32) Panagiotakos, D. B. Value of p-value in biomedical research. *Open Cardiovasc. Med. J.* **2008**, *2*, 97−99.
(33) Thomsen, V.; Schatzlein, D.; Mercuro, D. Limits of detection in spectroscopy. *Spectroscopy.* **2003**, *18* (12), 112−114.
(34) Min, C.-K.; Cheon, S.; Ha, N.-Y.; Sohn, K. M.; Kim, Y.; Aigerim, A.; Shin, H. M.; Choi, J.-Y.; Inn, K.-S.; Kim, J.-H. J. Comparative and kinetic analysis of viral shedding and immunological responses in MERS patients representing a broad spectrum of disease severity. *Sci. Rep.* **2016**, *6*, 25359.
(35) Kim, S.-K.; Sung, H.; Kim, M.-N. Kinetic Studies and Infection Control of Respiratory Viruses. *Korean J Healthc Assoc Infect Control Prev.* **2018**, *23* (1), 1−7.
(36) Al-Abdely, H. M.; Midgley, C. M.; Alkhamis, A. M.; Abedi, G. R.; Tamin, A.; Binder, A. M.; Alanazi, K.; Lu, X.; Abdalla, O.; Sakthivel, S. K. In *Infectious MERS-CoV Isolated From a Mildly Ill Patient, Saudi Arabia.*; Open Forum Infectious Diseases, Oxford University Press: US, 2018; p ofy111.
(37) Kraaij-Dirkzwager, M.; Timen, A.; Dirksen, K.; Gelinck, L.; Leyten, E.; Groeneveld, P.; Jansen, C.; Jonges, M.; Raj, S.; Thurkow, I. J. E., Middle East respiratory syndrome coronavirus (MERS-CoV) infections in two returning travellers in the Netherlands, May 2014, DOI: 10.2807/1560-7917.ES2014.19.21.20817.

DOI: 10.1021/acssensors.9b00175
ACS Sens. 2019, 4, 1306−1312